## Supporting Information

# A Colorimetric Plasmonic Nanosensor for Dosimetry of Therapeutic Levels of Ionizing Radiation

Karthik Pushpavanam[1], Eshwaran Narayanan[1], John Chang[2], Stephen Sapareto[2] and Kaushal Rege[1(*)]

[1] Chemical Engineering, Arizona State University, Tempe, AZ, 85287-6106

[2] Banner-MD Anderson Cancer Center, Gilbert, AZ, 85234

[(*)] To whom all correspondence must be addressed

Kaushal Rege
Chemical Engineering
501 E. Tyler Mall
ECG 301
Arizona State University
Tempe, AZ 85287-6106
Email: kaushal.rege@asu.edu
Phone: 480-727-8616
Fax: 480-727-9321

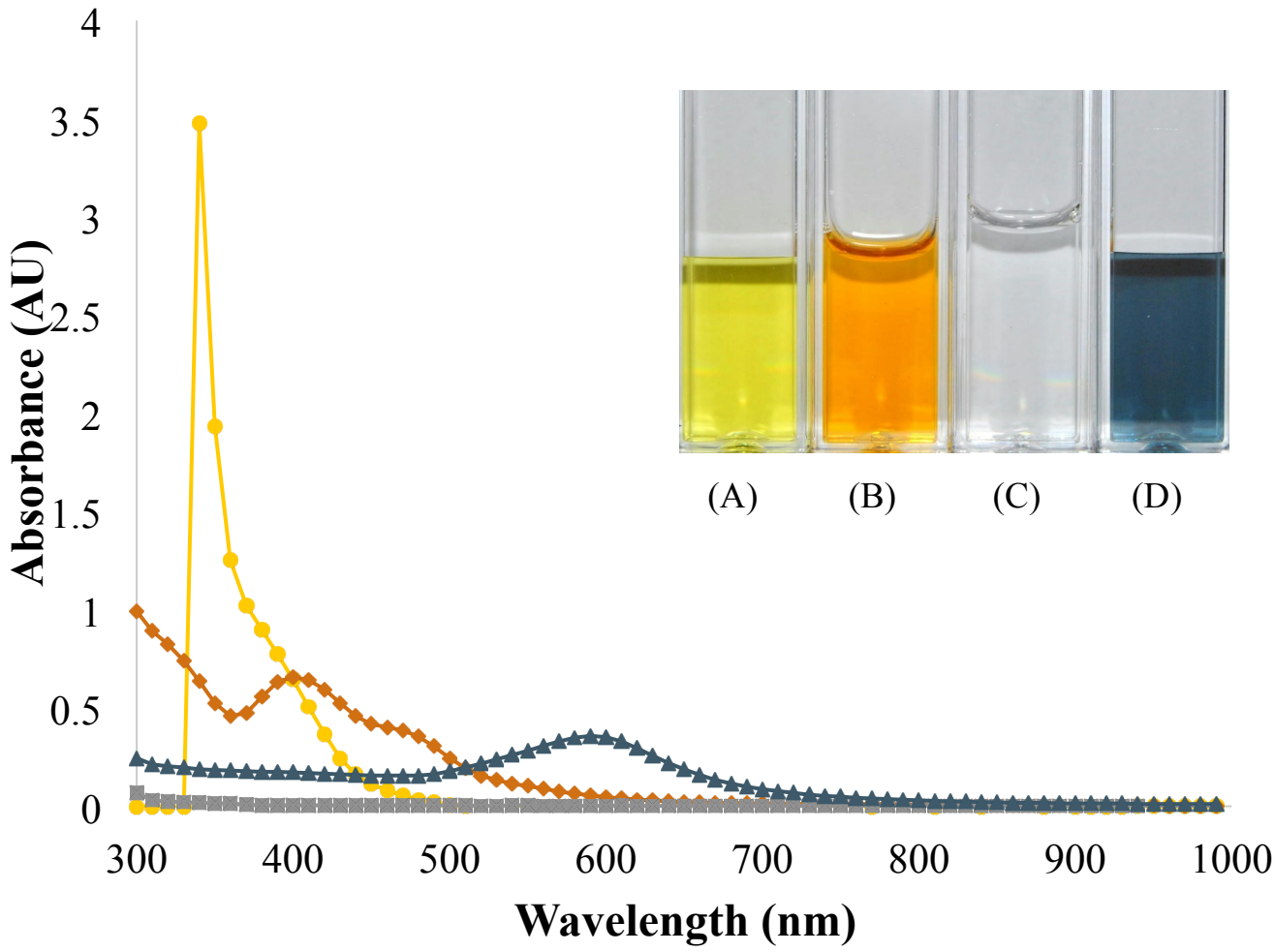


**Figure S1.** UV-visible wavelength spectral profiles of **(A)** $HAuCl_4$, **(B)** $HAuCl_4$ (0.196 mM) + $C_{16}TAB$ (20 mM), **(C)** $HAuCl_4$ (0.196 mM) + $C_{16}TAB$ (20 mM) + Ascorbic Acid (5.88 mM) and **(D)** $HAuCl_4$ (0.196 mM)+ Ascorbic Acid (5.88 mM).

A

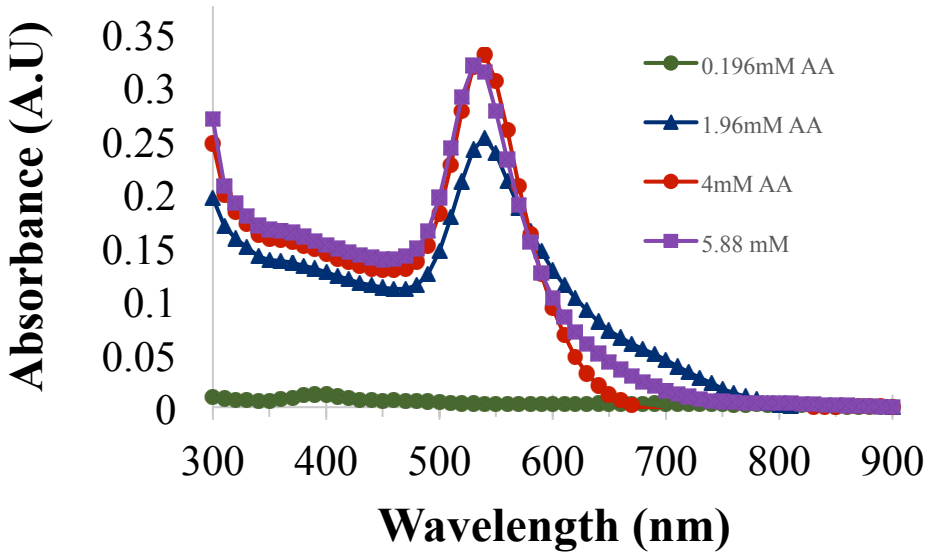


B

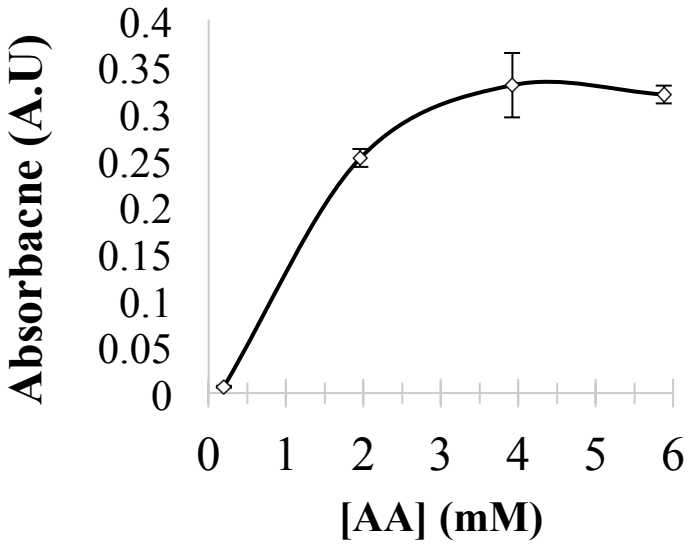


**Figure S2. (A)** UV-visible wavelength spectra of varying ascorbic acid volumes along with gold salt and $C_{16}$TAB solution irradiated at 47 Gy. A significant increase in the absorbance peak intensity is observed at ~520 nm when the amount of ascorbic acid is increased, indicating an increase in the formation of gold nanoparticles. **(B)** Maximum absorbance values of samples containing varying concentrations of ascorbic acid denoted as [AA].

A

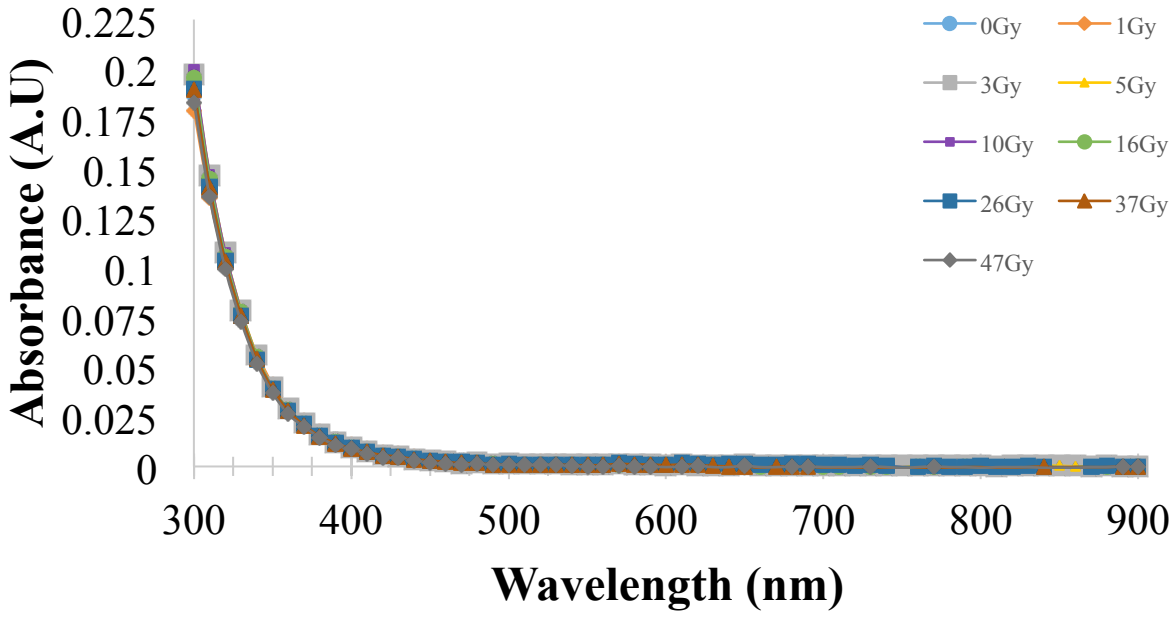
0.225
0.2
0.175
0.15
0.125
0.1
0.075
0.05
0.025
0
Absorbance (A.U)
300
400
500
600
700
800
900
Wavelength (nm)
0Gy
1Gy
3Gy
5Gy
10Gy
16Gy
26Gy
37Gy
47Gy

B

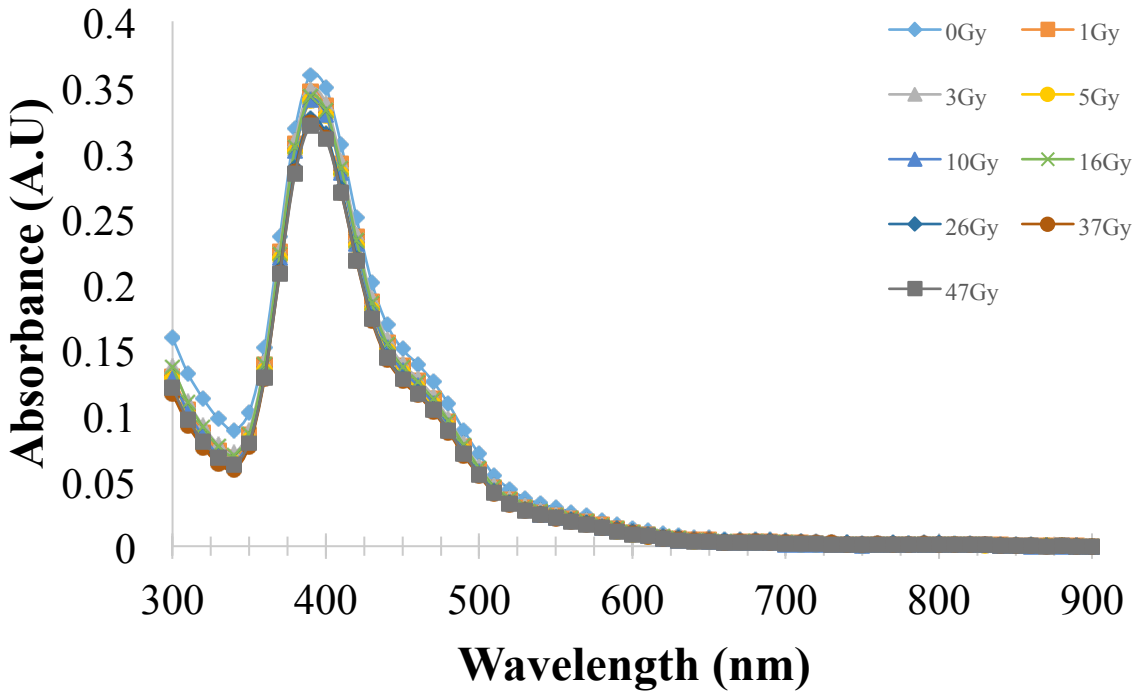
0.4
0.35
0.3
0.25
0.2
0.15
0.1
0.05
0
Absorbance (A.U)
300
400
500
600
700
800
900
Wavelength (nm)
0Gy
1Gy
3Gy
5Gy
10Gy
16Gy
26Gy
37Gy
47Gy

C

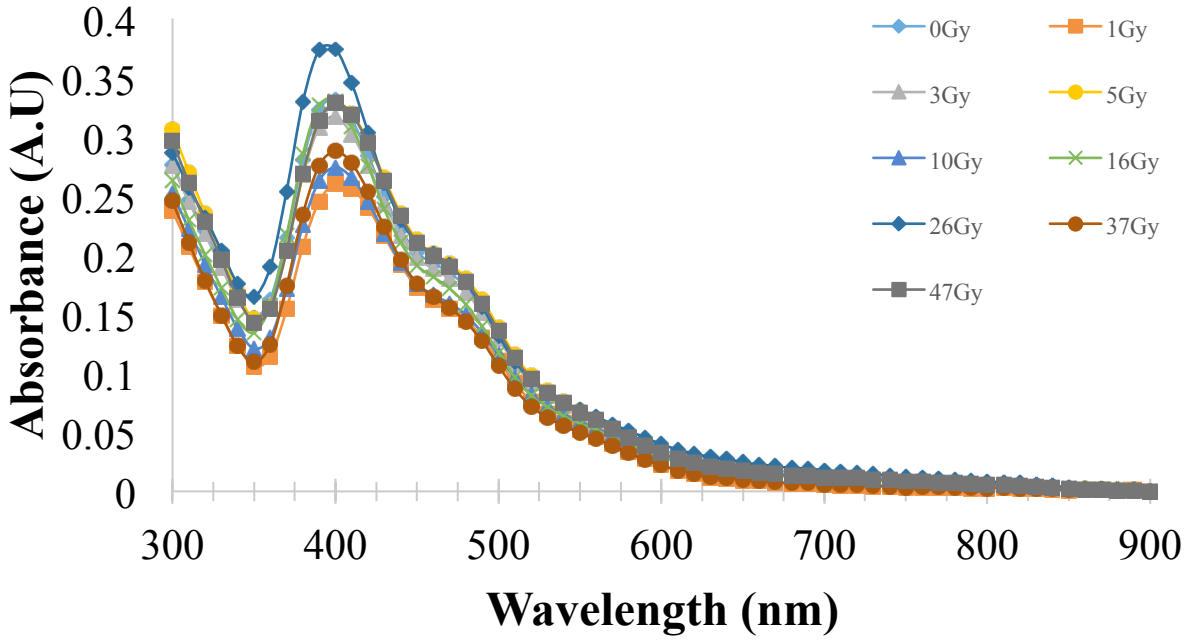


**Figure S3.** Absorbance spectra of **(A)** gold salt (0.196 mM) **(B)** gold salt (0.196 mM) + $C_{16}$TAB (20 mM) **(C)** gold salt (0.196 mM) + $C_{12}$TAB (20 mM) treated with different doses of X-ray radiation. Nanoparticle formation, as indicated by a plasmonic peak at ca. 520 nm, is not observed in the absence of ascorbic acid signifying its importance in the plasmonic nanosensor system.

A

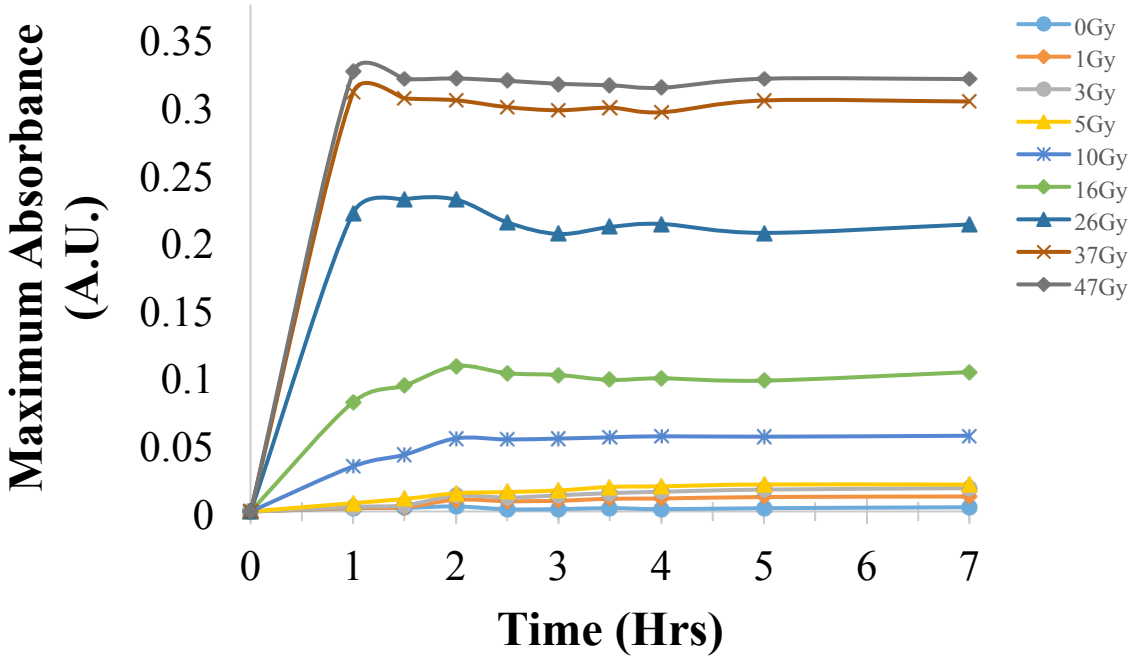
Maximum Absorbance (A.U.)
0.35
0.3
0.25
0.2
0.15
0.1
0.05
0
0
1
2
3
4
5
6
7
Time (Hrs)
0Gy
1Gy
3Gy
5Gy
10Gy
16Gy
26Gy
37Gy
47Gy

B

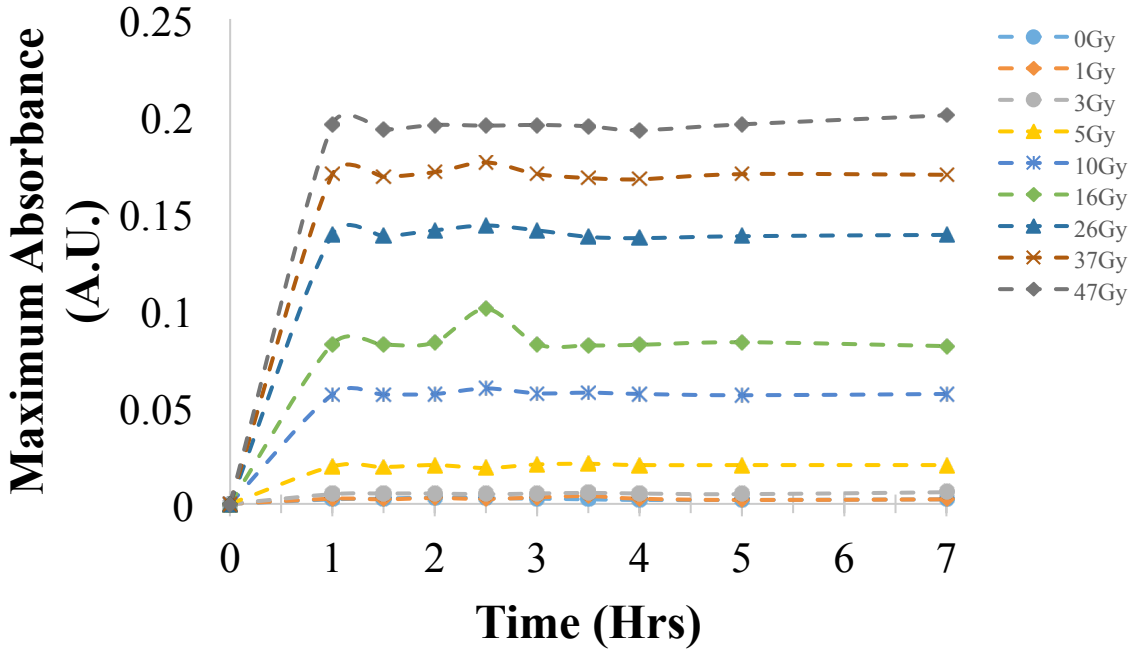
Maximum Absorbance (A.U.)
0.25
0.2
0.15
0.1
0.05
0
0
1
2
3
4
5
6
7
Time (Hrs)
0Gy
1Gy
3Gy
5Gy
10Gy
16Gy
26Gy
37Gy
47Gy

C

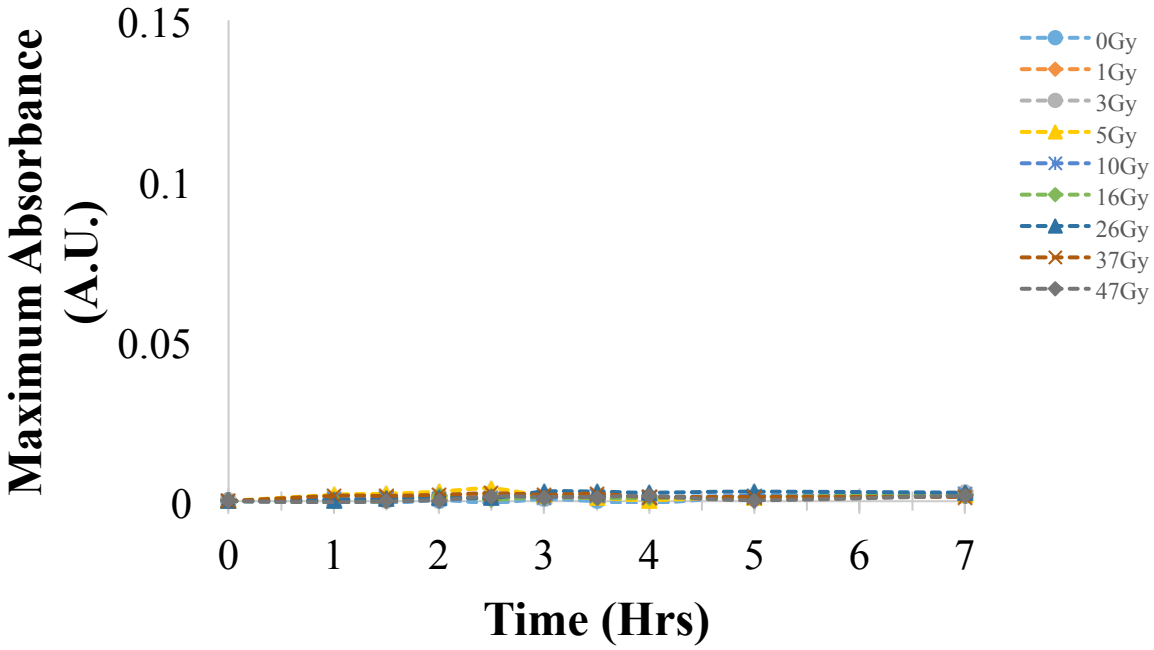


**Figure S4.** Kinetics of gold nanoparticle formation following exposure to different doses of ionizing radiation (0-47 Gy) for **(A)** $C_{16}$TAB, **(B)** $C_{12}$TAB and **(C)** $C_8$TAB. Maximum (peak) absorbance values, typically between 450 nm and 650 nm, are plotted as a function of time following irradiation. The maximal value is reached at 1 h in most cases, but requires up to 2 h for lower doses. The value remains unchanged over a period of 7 h. The lipid concentration was 20 mM in each case.

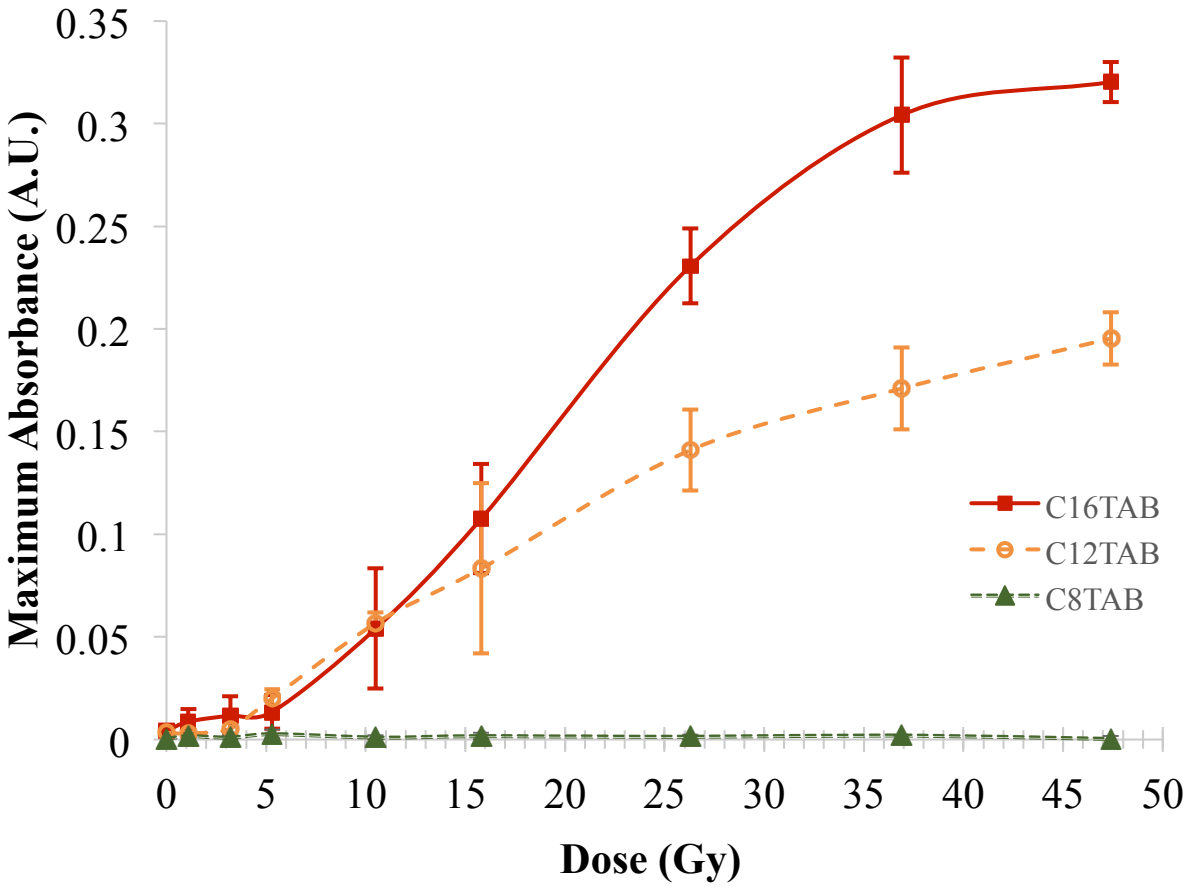


**Figure S5.** Maximum absorbance vs. radiation dose (Gy) after 2 hours of X-ray irradiation. $C_{16}$TAB (red filled squares, solid line) and $C_{12}$TAB (orange open circles, dotted line) surfactants. $C_8$TAB (green triangles, dotted line) does not show any response to radiation. The lipid concentration was 20 mM in all cases.

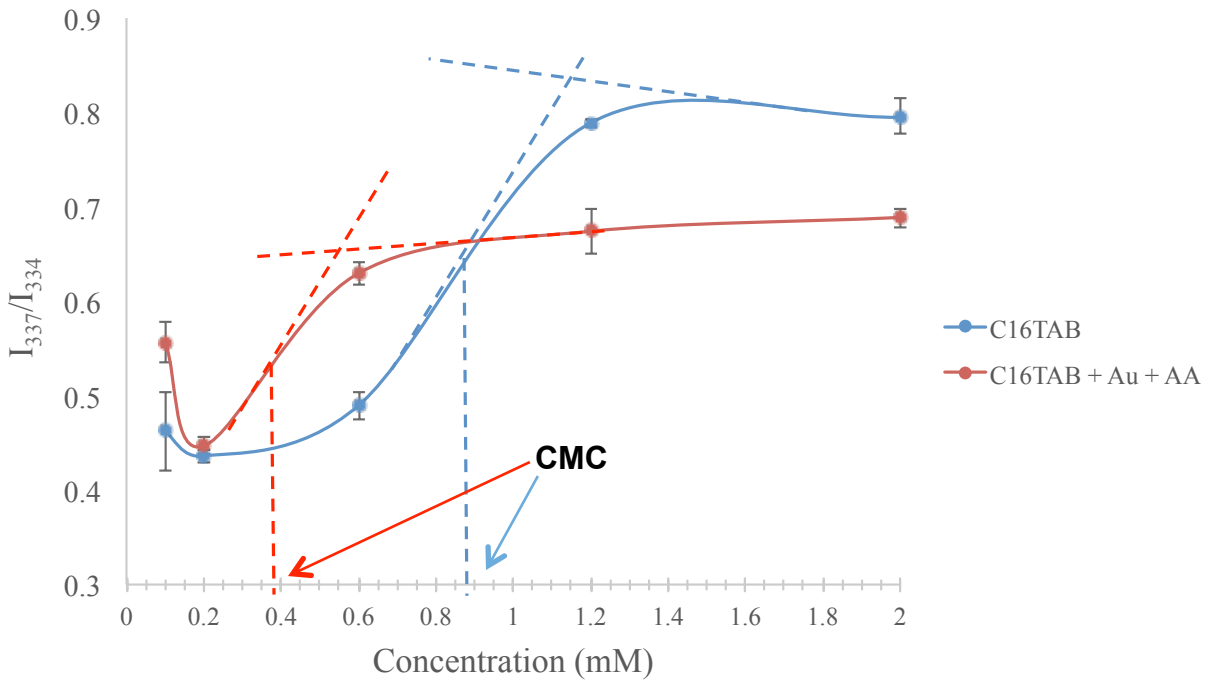


**Figure S6.** Determination of the critical micelle concentration (CMC) value for $C_{16}$TAB in the nanosensor precursor solution ('C16TAB + Au + AA' in the legend) and DI Water ('C16TAB' in the legend) using the pyrene fluorescence assay. The intensity ratio of $I_{337}/I_{334}$ was plotted as a function of the lipid surfactant concentration and the CMC value was determined from the mid-point as shown in the figure. The dashed lines are for visualization alone. n = 2 independent experiments. Spontaneous nanoparticle formation was seen with the nanosensor precursor solution at 0.1 mM resulting in increased fluorescence intensity at this condition. As seen in the figure, the CMC of $C_{16}$TAB was ~0.88 mM and that for $C_{16}$TAB in the nanosensor precursor solution was ~0.39 mM.

**A**

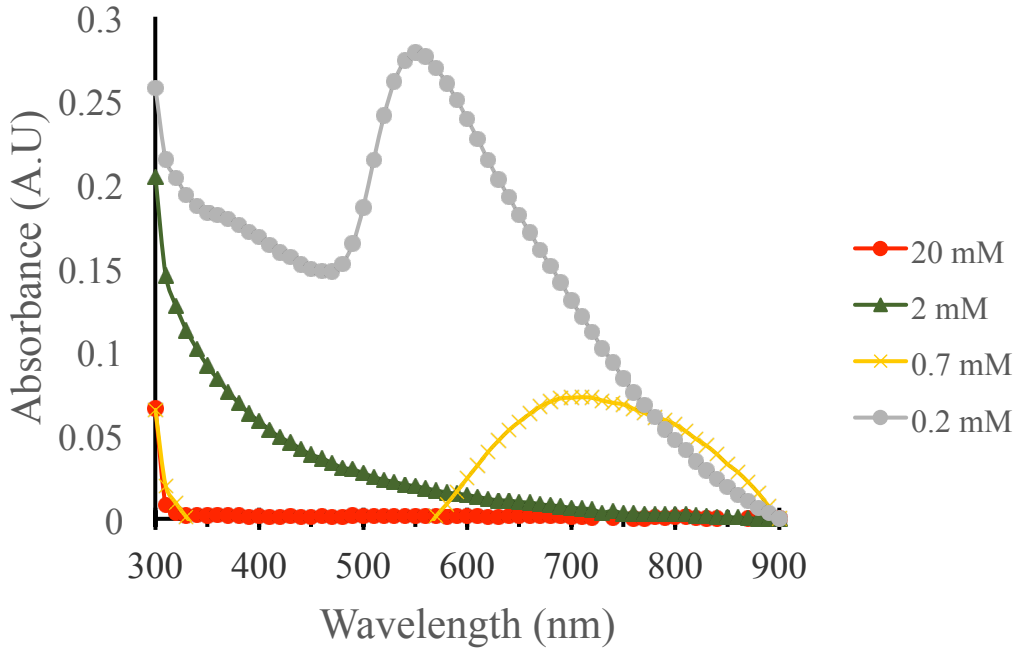
0.3
0.25
0.2
0.15
0.1
0.05
0
Absorbance (A.U)
300
400
500
600
700
800
900
Wavelength (nm)
20 mM
2 mM
0.7 mM
0.2 mM

**B**

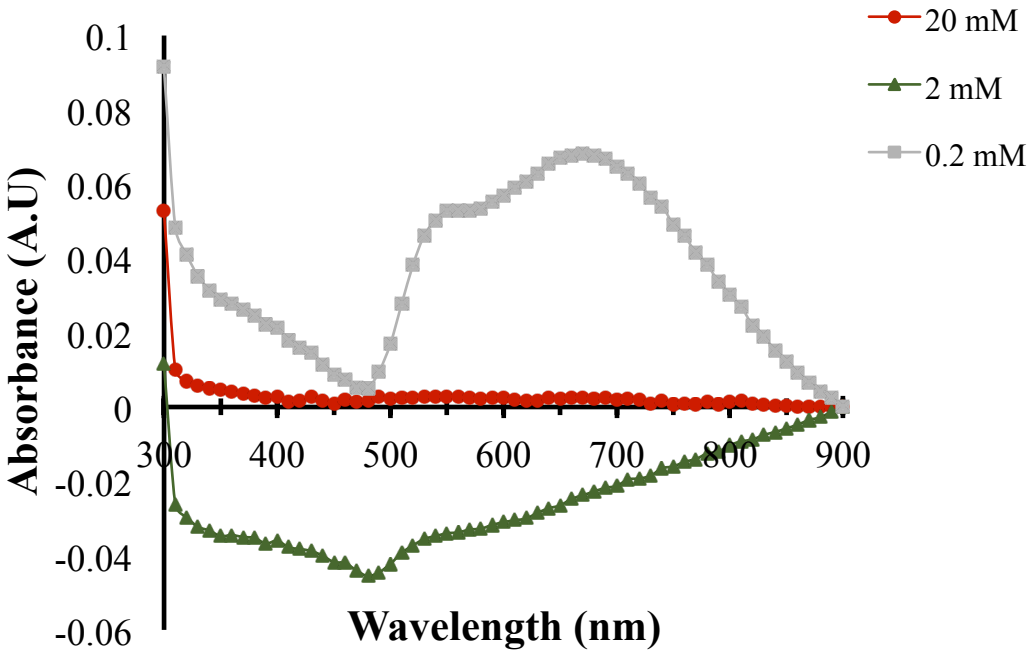
0.1
0.08
0.06
0.04
0.02
0
-0.02
-0.04
-0.06
Absorbance (A.U)
300
400
500
600
700
800
900
Wavelength (nm)
20 mM
2 mM
0.2 mM

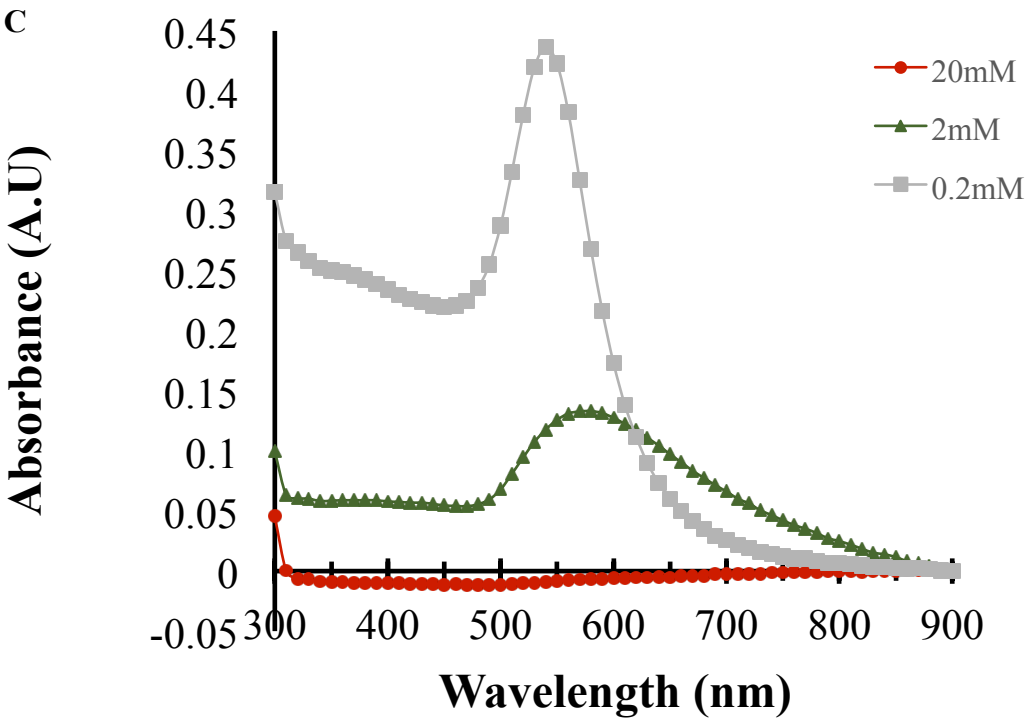


**Figure S7.** Absorbance spectra of precursor monovalent gold salt solutions under conditions of no radiation (i.e. 0 Gy) in presence of different concentrations of **(A)** $C_{16}$TAB and **(B)** $C_{12}$TAB **(C)** $C_8$TAB recorded after 10 minutes of incubation. Spontaneous nanoparticle formation was seen at 0.2 mM for all lipid surfactants, as indicated by the characteristic absorbance peak of gold nanoparticles at ~520 nm. In contrast, no nanoparticle formation was observed at a lipid concentration of 20 mM for up to 7 h.

A

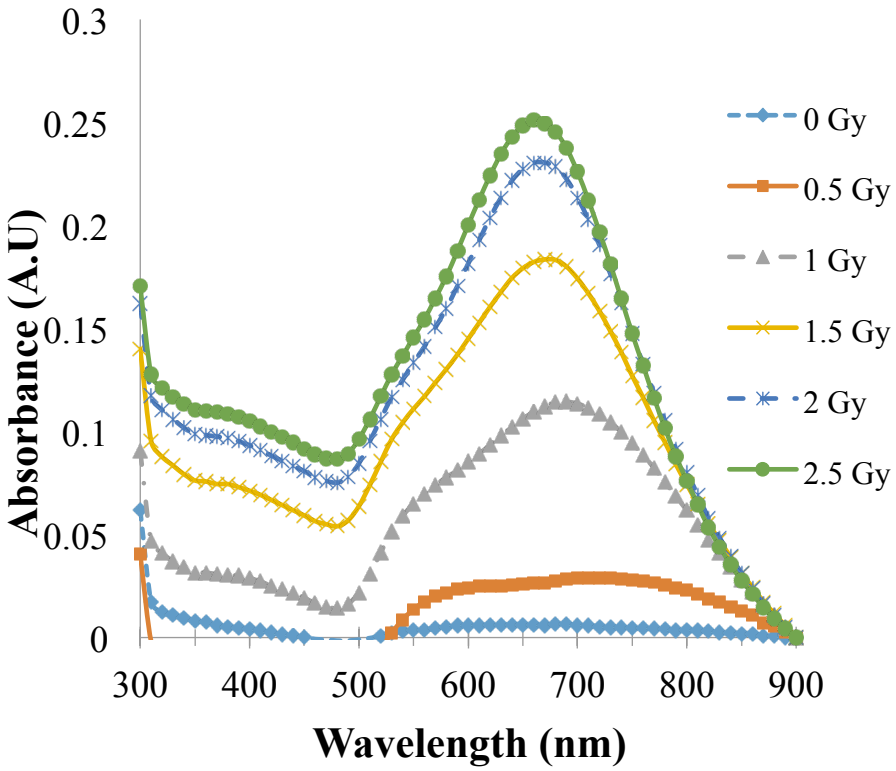
0.3
0.25
0.2
0.15
0.1
0.05
0
Absorbance (A.U)
300
400
500
600
700
800
900
Wavelength (nm)
0 Gy
0.5 Gy
1 Gy
1.5 Gy
2 Gy
2.5 Gy

B

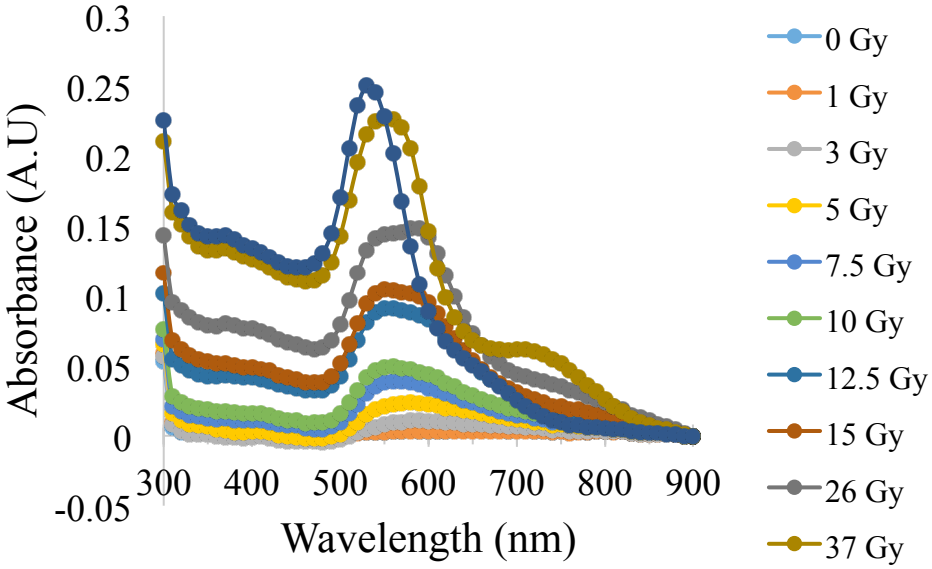
0.3
0.25
0.2
0.15
0.1
0.05
0
-0.05
Absorbance (A.U)
300
400
500
600
700
800
900
Wavelength (nm)
0 Gy
1 Gy
3 Gy
5 Gy
7.5 Gy
10 Gy
12.5 Gy
15 Gy
26 Gy
37 Gy

C

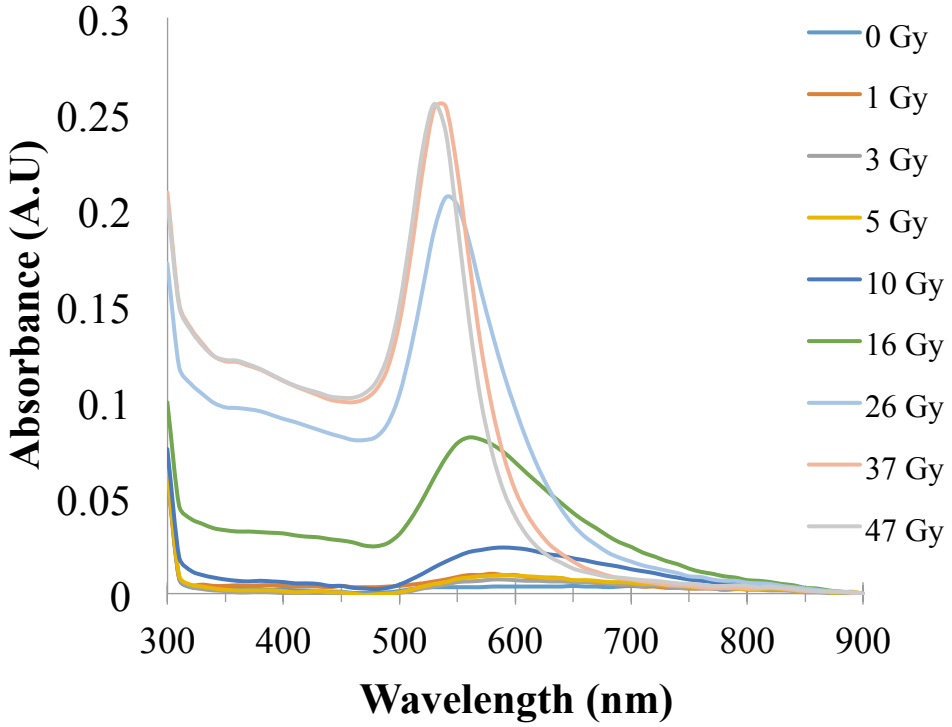


D

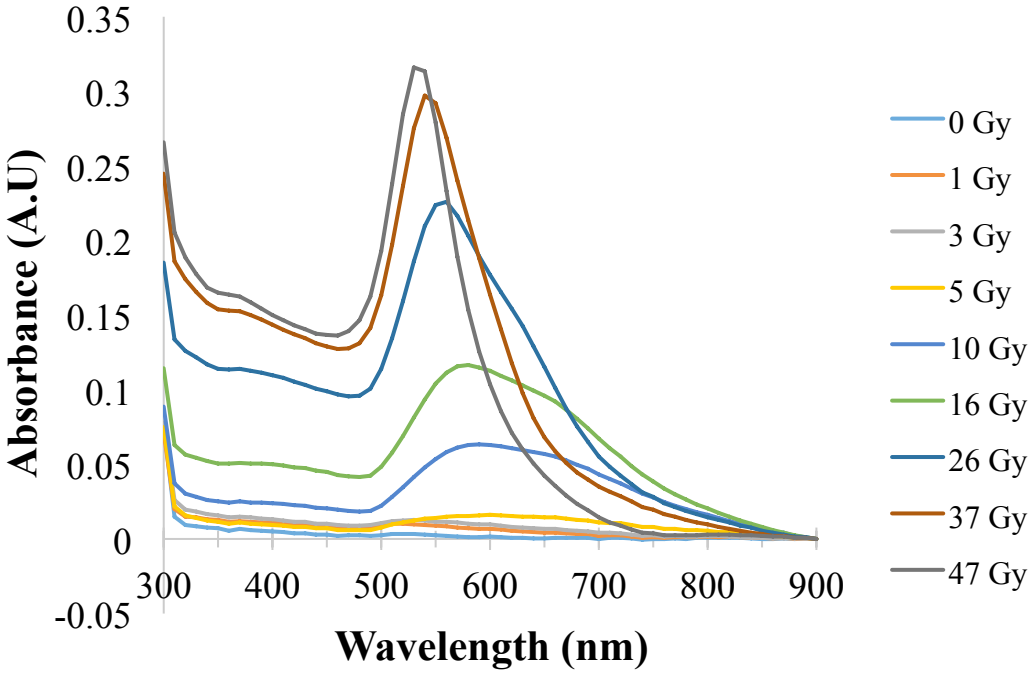


**Figure S8.** Maximum absorbance vs. wavelength for different concentrations of $C_{16}$TAB after a duration of 2 hours post irradiation with different doses of X-rays. **(A)** 2mM **(B)** 4mM **(C)** 10mM **(D)** 20mM $C_{16}$TAB.

A

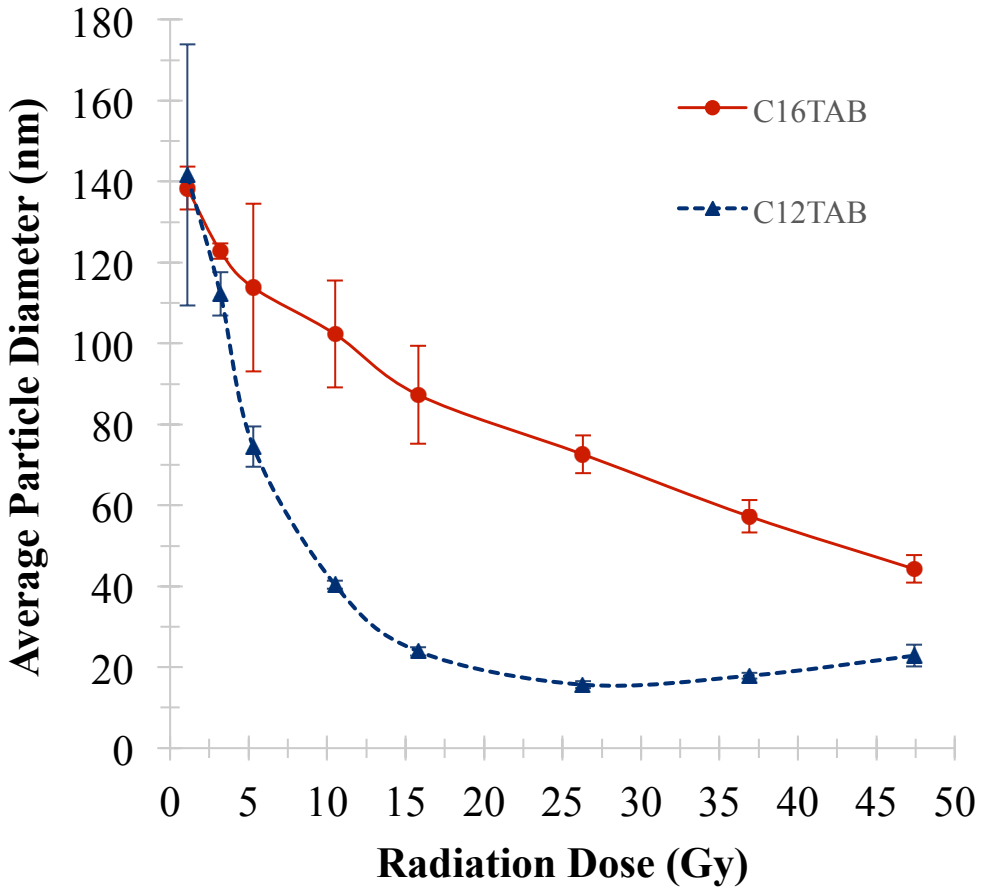
Average Particle Diameter (nm)
180
160
140
120
100
80
60
40
20
0
0
5
10
15
20
25
30
35
40
45
50
Radiation Dose (Gy)
C16TAB
C12TAB

B

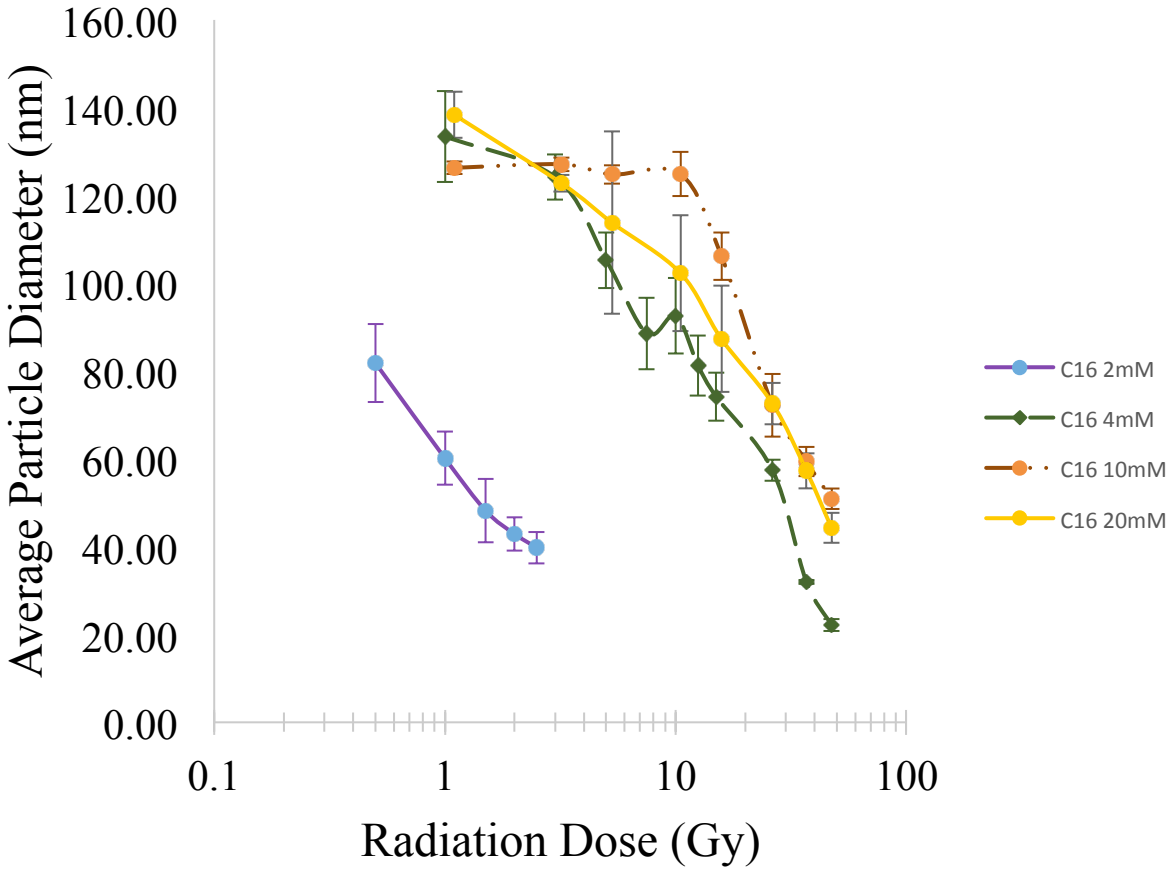


**Figure S9. (A)** Nanoparticle hydrodynamic diameter vs. radiation dose. An increase in average particle diameter is observed with a decrease in radiation dose for both 20 mM $C_{16}$TAB (red circles) and 20 mM $C_{12}$TAB (blue triangles). **(B)** Hydrodynamic diameter vs. radiation dose for different concentrations of $C_{16}$TAB (plotted on a $\log_{10}$ scale on the X-axis). An increase in average particle diameter is observed with a decrease in radiation dose for all four different concentration of $C_{16}$TAB employed. Blue circles: 2mM; green diamonds: 4mM; orange circles: 10mM and yellow circles: 20mM $C_{16}$TAB.

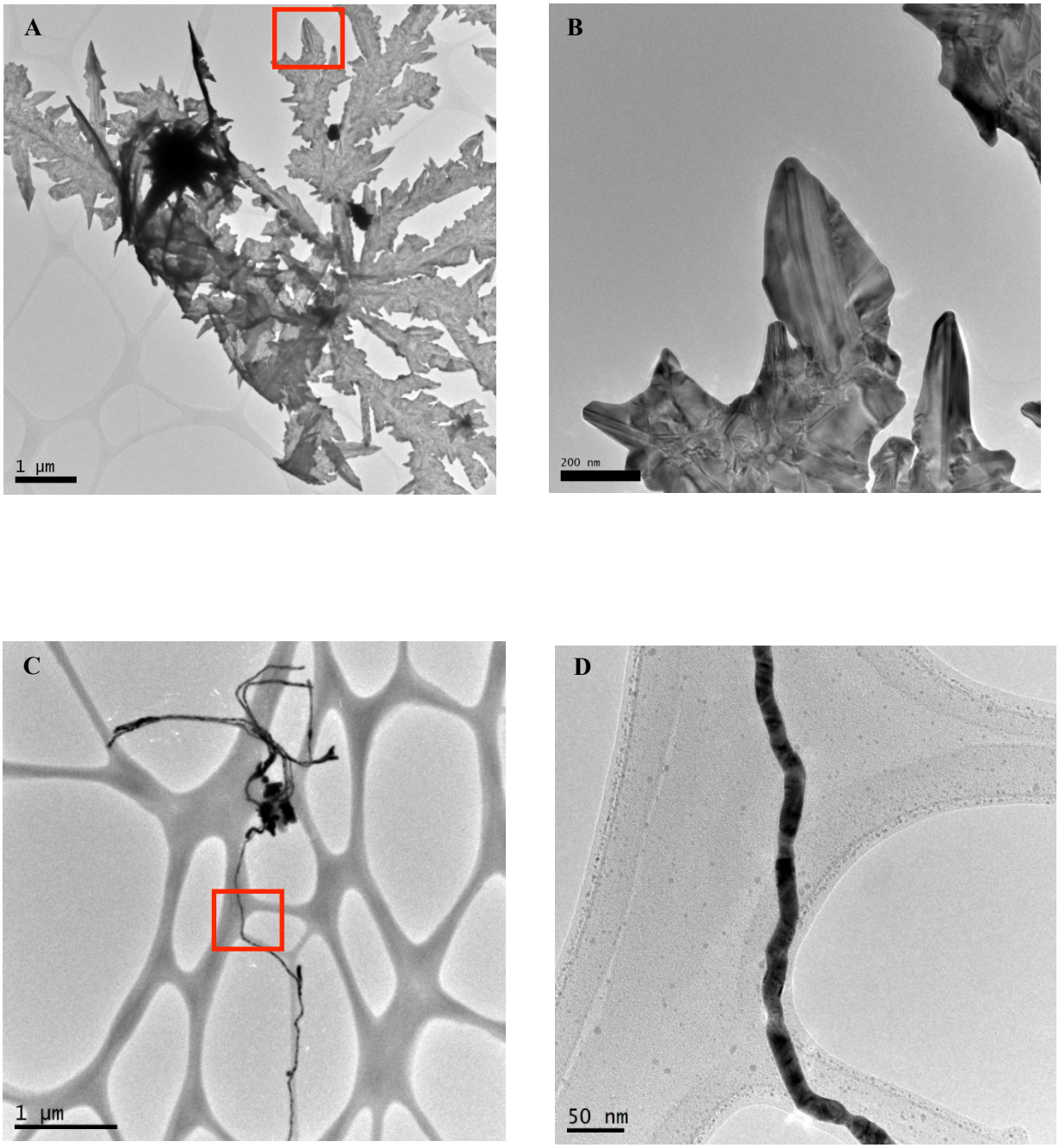


**Figure S10.** Transmission electron microscopy (TEM) images of anisotropic nanostructures **(A)** dendritic and **(C)** nanowire-like structures formed in case of $C_{12}$TAB at 5 Gy X-ray radiation dose. Images **(B)** and **(D)** show magnified images of the highlighted regions inside red box from Figures **(A)** and **(C)**.

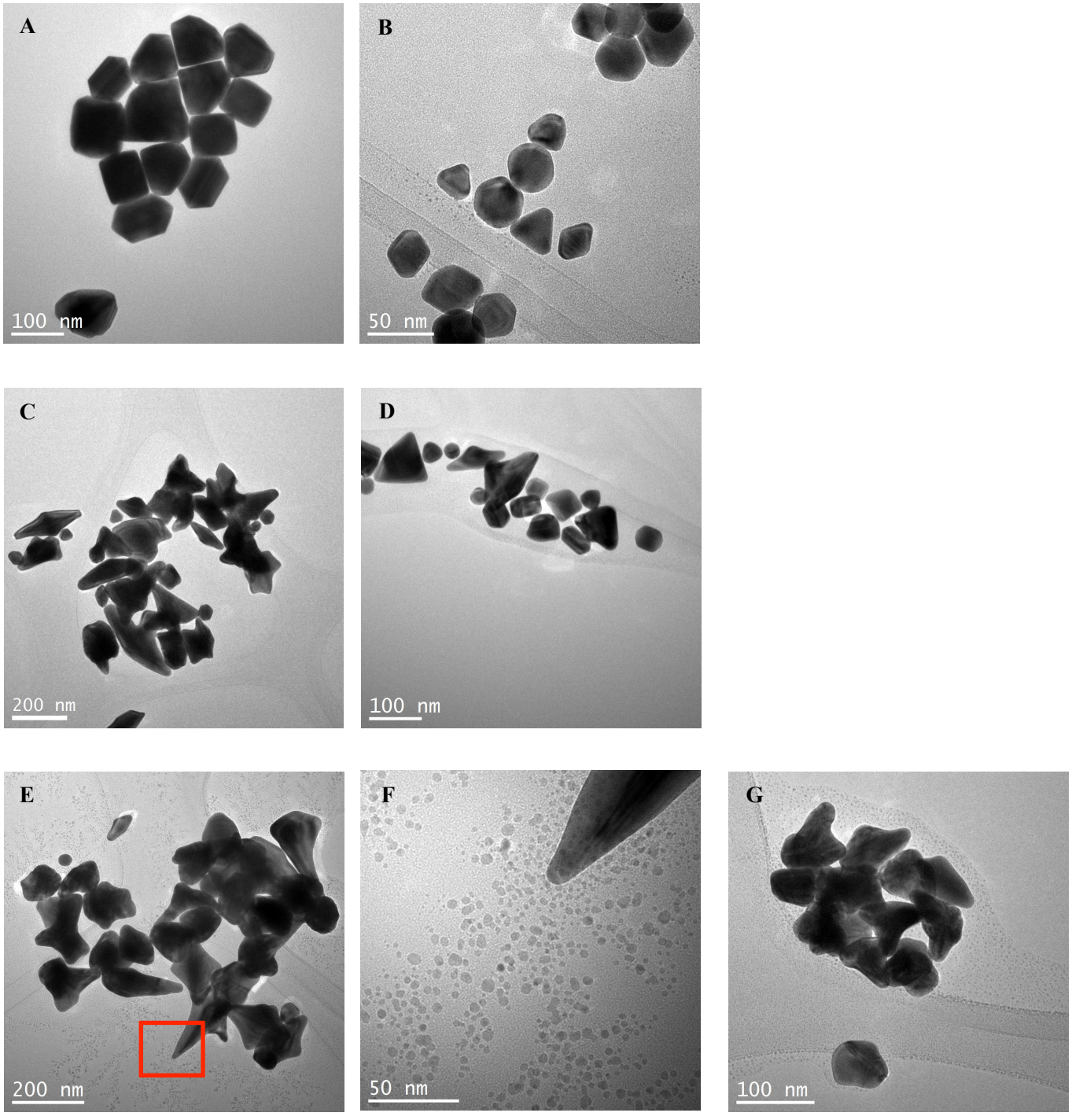


**Figure S11.** Transmission Electron Microscopy (TEM) images of gold nanoparticles formed after exposure to ionizing (X-ray) radiation using the following conditions of $C_{16}$TAB. **(A)** 10 mM and 5 Gy, **(B)** 10 mM and 47 Gy, **(C)** 4 mM and 5 Gy, **(D)** 4 mM and 15 Gy**, (E)** 2 mM and 0.5 Gy, **(F)** Magnified image of highlighted area of **E** showing smaller particles**,** and **(G)** 2 mM and 2.5 Gy.

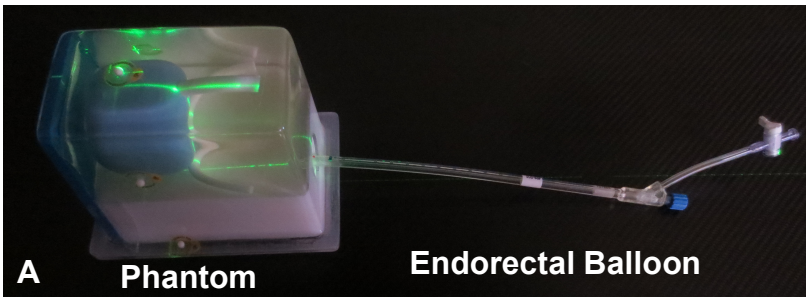


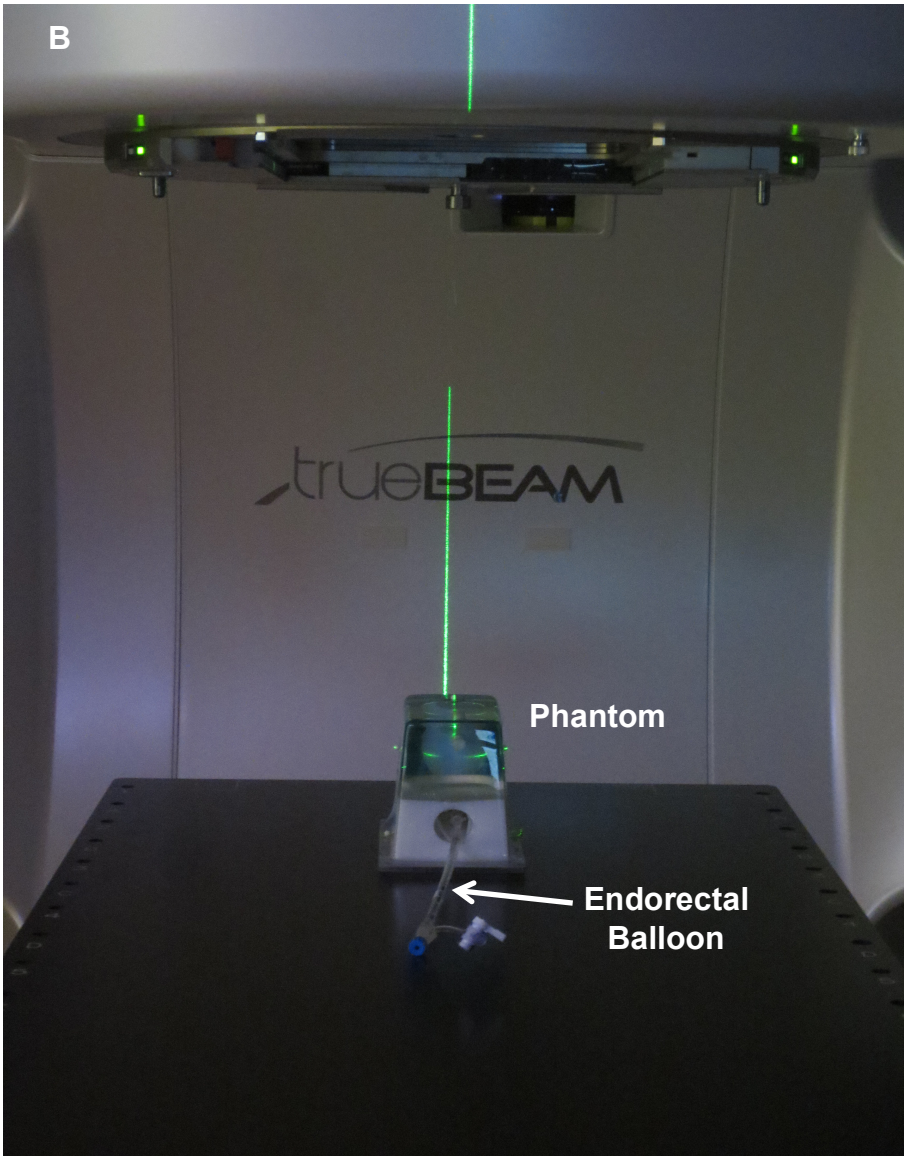


**Figure S12.** Digital images showing the anthropomorphic prostate phantom irradiation set up on the linear accelerator at the Banner-MD Anderson Cancer Center in Gilbert, AZ. (A) Top view and (B) front-on / side view.

| Surfactant | Dose | Average Diameter (nm) | Standard Deviation Diameter (nm) | Average Polydispersity Index(PDI) |
|---|---|---|---|---|
| $C_{16}$ 20mM | 1 Gy | 138.4 | 5.3 | 0.2 |
| | 3 Gy | 122.8 | 1.9 | 0.2 |
| | 5 Gy | 121.1 | 20.7 | 0.3 |
| | 10 Gy | 102.3 | 13.2 | 0.2 |
| | 16 Gy | 88.5 | 12.1 | 0.2 |
| | 26 Gy | 72.6 | 4.7 | 0.2 |
| | 37 Gy | 57.3 | 4.0 | 0.3 |
| | 47 Gy | 45.5 | 3.4 | 0.3 |
| | | | | |
| $C_{16}$ 2mM | 0.5 Gy | 81.9 | 8.9 | 0.3 |
| | 1 Gy | 60.2 | 6.1 | 0.3 |
| | 1.5 Gy | 48.2 | 7.3 | 0.4 |
| | 2 Gy | 42.9 | 3.8 | 0.4 |
| | 2.5 Gy | 39.8 | 3.6 | 0.4 |
| | | | | |
| $C_{16}$ 4mM | 1 Gy | 133.4 | 10.4 | 0.2 |
| | 3 Gy | 124.2 | 5.2 | 0.2 |
| | 5 Gy | 105.3 | 6.3 | 0.2 |
| | 7.5 Gy | 88.6 | 8.1 | 0.3 |
| | 10 Gy | 92.6 | 8.6 | 0.3 |
| | 12.5 Gy | 81.3 | 6.9 | 0.3 |
| | 15 Gy | 74.2 | 5.5 | 0.3 |
| | 26 Gy | 57.4 | 2.4 | 0.3 |
| | 37 Gy | 32.0 | 0.4 | 0.5 |
| | 47 Gy | 22.1 | 1.3 | 0.6 |
| | | | | |
| $C_{16}$ 10mM | 1 Gy | 126.4 | 1.5 | 0.2 |
| | 3 Gy | 127.1 | 1.6 | 0.2 |
| | 5 Gy | 124.8 | 2.1 | 0.2 |
| | 10 Gy | 124.9 | 5.0 | 0.2 |
| | 16 Gy | 106.2 | 5.4 | 0.2 |
| | 26 Gy | 72.2 | 7.1 | 0.2 |
| | 37 Gy | 59.4 | 3.3 | 0.3 |

| | | | | |
|---|---|---|---|---|
| | 47 Gy | 50.9 | 2.3 | 0.2 |
| | | | | |
| $C_{12}$ 20mM | 1 Gy | 141.6 | 32.2 | 0.5 |
| | 3 Gy | 112.2 | 5.3 | 0.2 |
| | 5 Gy | 75.2 | 5.0 | 0.3 |
| | 10 Gy | 40.4 | 1.0 | 0.5 |
| | 16 Gy | 23.9 | 1.1 | 0.6 |
| | 26 Gy | 15.7 | 0.8 | 0.6 |
| | 37 Gy | 17.9 | 0.7 | 0.6 |
| | 47 Gy | 21.6 | 2.7 | 0.6 |

**Table S1.** Average hydrodynamic diameters of gold nanoparticles formed after irradiation along with their corresponding polydispersity indices.